



CATHODE MATERIALS FOR NEXT GENERATION LITHIUM-ION BATTERIES: THEORY AND MODELING OF LOW-COBALT CATHODES

Project ID: BAT253

HAKIM IDDIR

Argonne National Laboratory
June 21-23, 2022

2022 DOE Vehicle Technologies Office
Annual Merit Review

Relevance

Geopolitical concerns over critical resources, and in particular cobalt, as well as market demand have instigated new efforts to improve the sustainability of lithium-ion cathode technologies. This project will use first-principles modeling applied to prototypical cobalt free cathode oxides including LiNiO_2 (LNO), $\text{LiNi}_{0.5}\text{Mn}_{0.5}\text{O}_2$, and newly developed derivatives thereof in order to advance cathode design in accord with DOE targets for cost, performance, and sustainability

Project Goals

- Identify promising surface and bulk, dopant elements and provide a fundamental understanding of their efficacy in modifying the properties low/no cobalt oxides with respect to cobalt as a counterpart.
- Gain understanding on how earth abundant (EA) elements affect Li-Mn rich materials ordering/domains/structure/morphology and the influence on the material properties and reactivity.
- Obtain design insights for advanced oxide cathodes through model-system based studies
- Synthesize and develop next-generation materials based on the obtained knowledge

Overview

Timeline

- Start: October 1, 2018
- End: September 30, 2022
- Percent complete: 90%

Budget

- Total project funding:
FY22 \$4.0M
- ANL, NREL, ORNL, LBNL, PNNL

Barriers

- Development of PHEV and EV batteries that meet or exceed DOE and USABC goals
 - Cost
 - Performance
 - Safety
 - Cobalt content

Partners

- ANL, NREL, ORNL, LBNL, PNNL

Students supported from:

- University of Illinois at Chicago
- University of Rochester
- Oregon State University
- Worcester Polytechnic Institute

Milestones

Theory

- Determine site preference and ordering for earth abundant elements in $\text{Li}_2\text{MnO}_3\text{-LiMn}_{0.5}\text{Ni}_{0.5}\text{O}_2$ using Density Functional Theory (*Q1: accomplished*)
- Evaluate the effect of earth abundant (EA) candidates on Li-M exchange (M=Ni, Mn, EA), structure stability at high states of charge (*Q2-Q3: on track*)
- Evaluate the effect of earth abundant (EA) candidates on particle morphology and surface reactivity (*Q4*)

Model Systems

- Develop single-crystal models for studying factors controlling F incorporation, surface vs. bulk distribution
- Investigate the effect of synthesis parameters on F incorporation

Approach

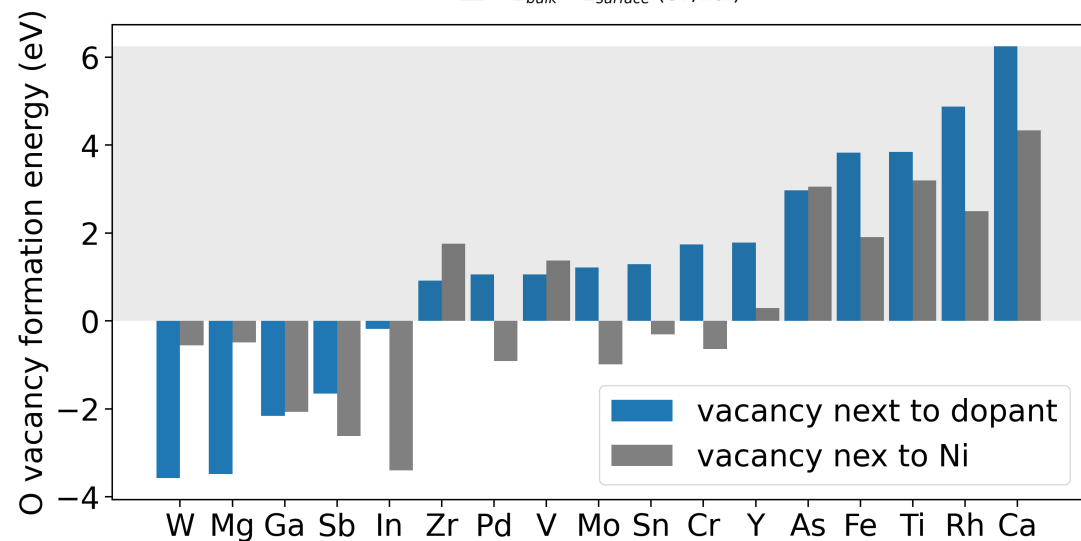
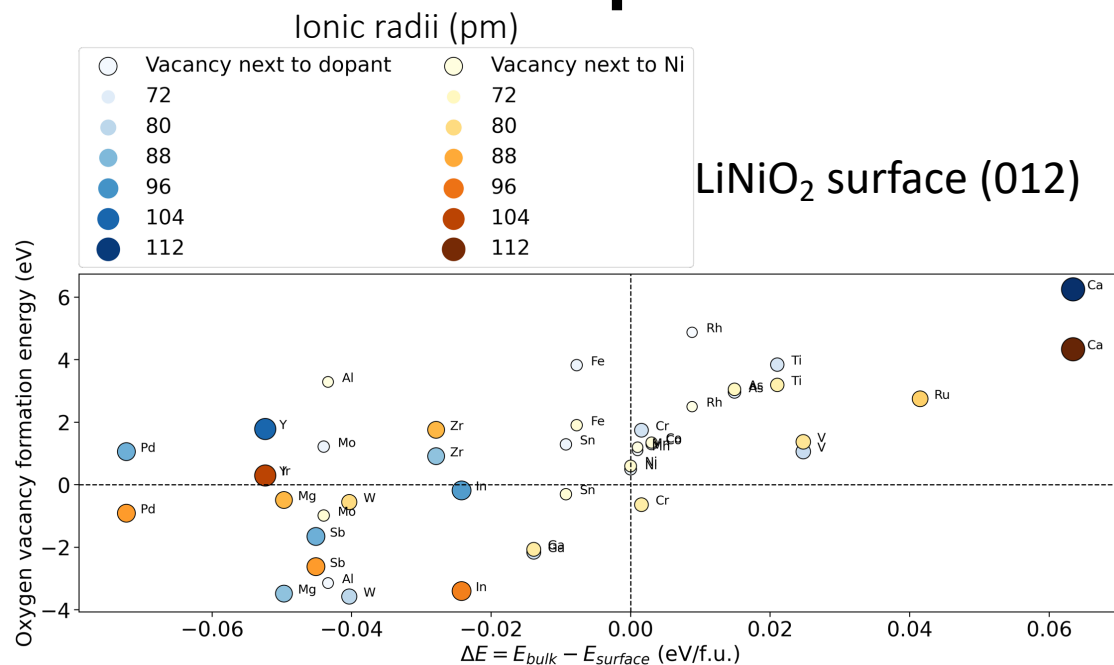
Theory

- Perform atomistic modeling at the DFT level in order to gain understanding on Li ion batteries and provide physical properties for multi scale modeling
- Work in close collaboration with synthesis and characterization for the design of new materials
- Use $\text{Li}_2\text{MnO}_3\text{-LiMn}_{0.5}\text{Ni}_{0.5}\text{O}_2$ as a base composition
- Substitute Ni with EA elements in $\text{Li}_2\text{MnO}_3\text{-LiMn}_{0.5}\text{Ni}_{0.5}\text{O}_2$ and create diverse cation configurations to evaluate:
 - Site preference for earth abundant
 - Li_2MnO_3 domains size change
 - Electronic properties using Density functional theory

Model Systems

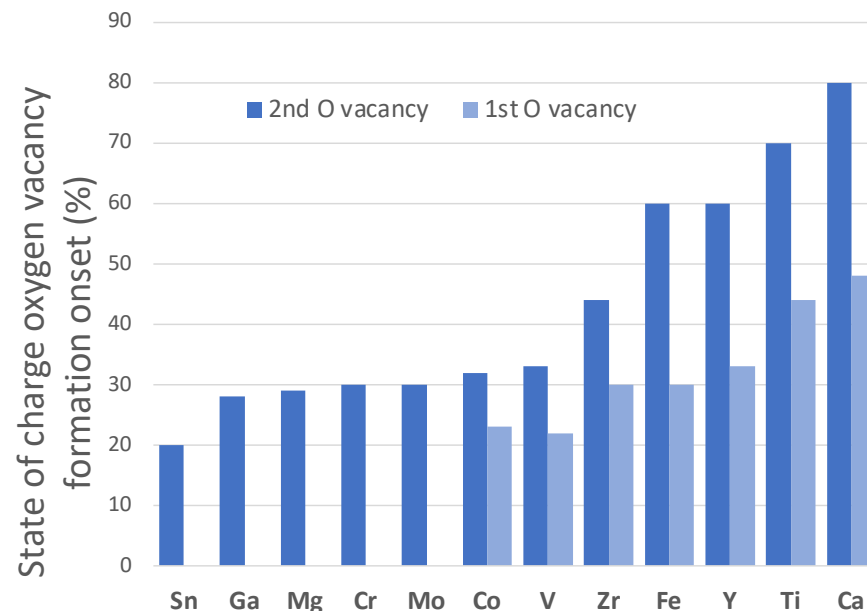
- Synthesize well-formed single-crystal models
- Use advanced diagnostic techniques to gain understanding of properties - processes - performance correlations in oxide cathodes
- Design and develop advanced materials based on the obtained knowledge

Technical Accomplishments



Dopants that prefer surface sites, render the surface less reactive, hence should improve cathode performance

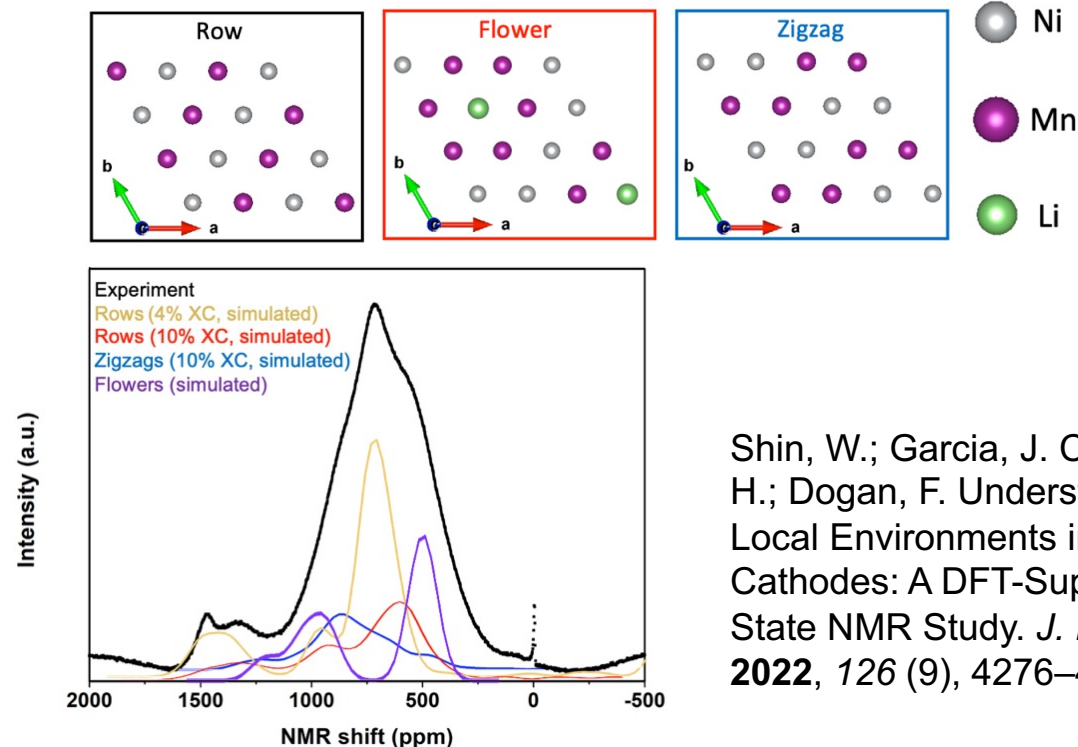
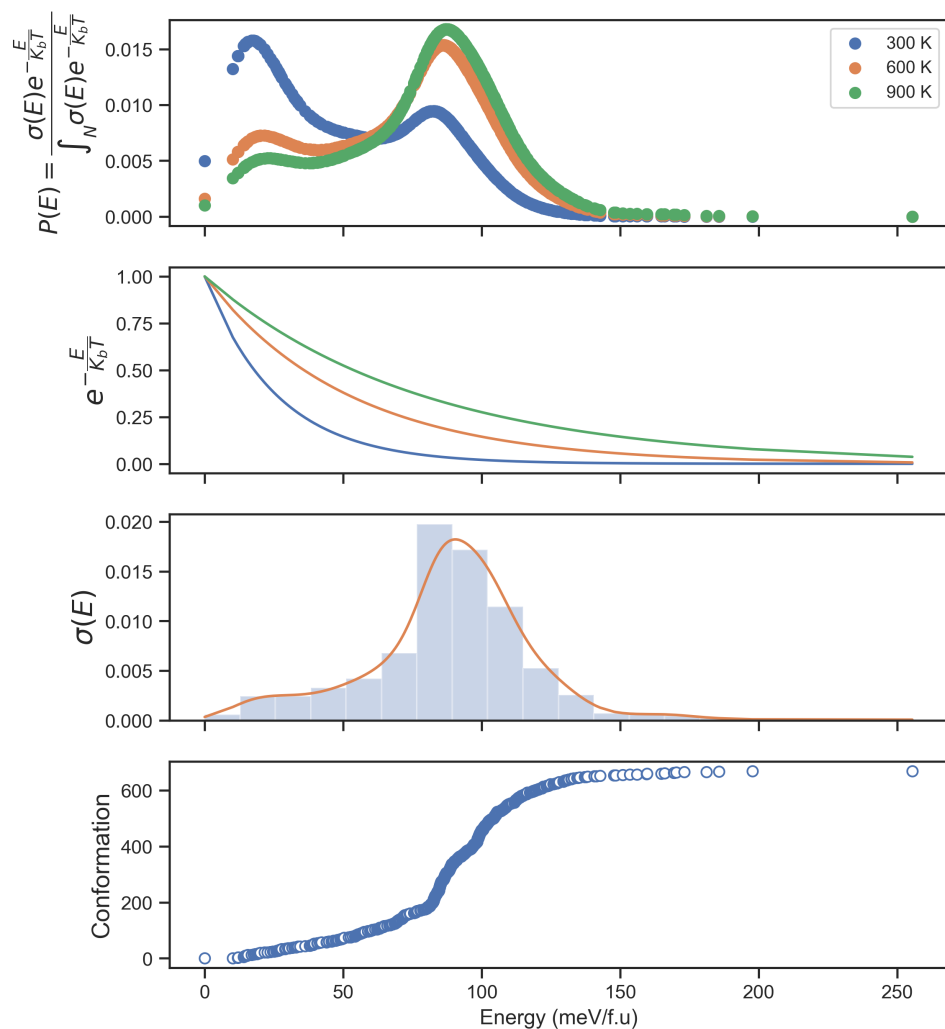
LiNiO₂: Active surfaces-Oxygen loss-Dopants



- The LiNiO₂ (012) surface is the most abundant, reactive and sensitive to the presence of dopants as shown in the figures
- The most effective dopants against oxygen reactivity and loss prefer the surface sites and have a positive oxygen vacancy formation energy (proxy for reactivity)
- The (104) surface is less abundant and less reactive. All the dopants investigated so far further improve its stability

Technical Accomplishments

LiNi_{0.5}Mn_{0.5}O₂: Structure-NMR



Shin, W.; Garcia, J. C.; Vu, A.; Ji, X.; Iddir, H.; Dogan, F. Understanding Lithium Local Environments in LiMn_{0.5}Ni_{0.5}O₂ Cathodes: A DFT-Supported 6Li Solid-State NMR Study. *J. Phys. Chem. C* **2022**, 126 (9), 4276–4285.

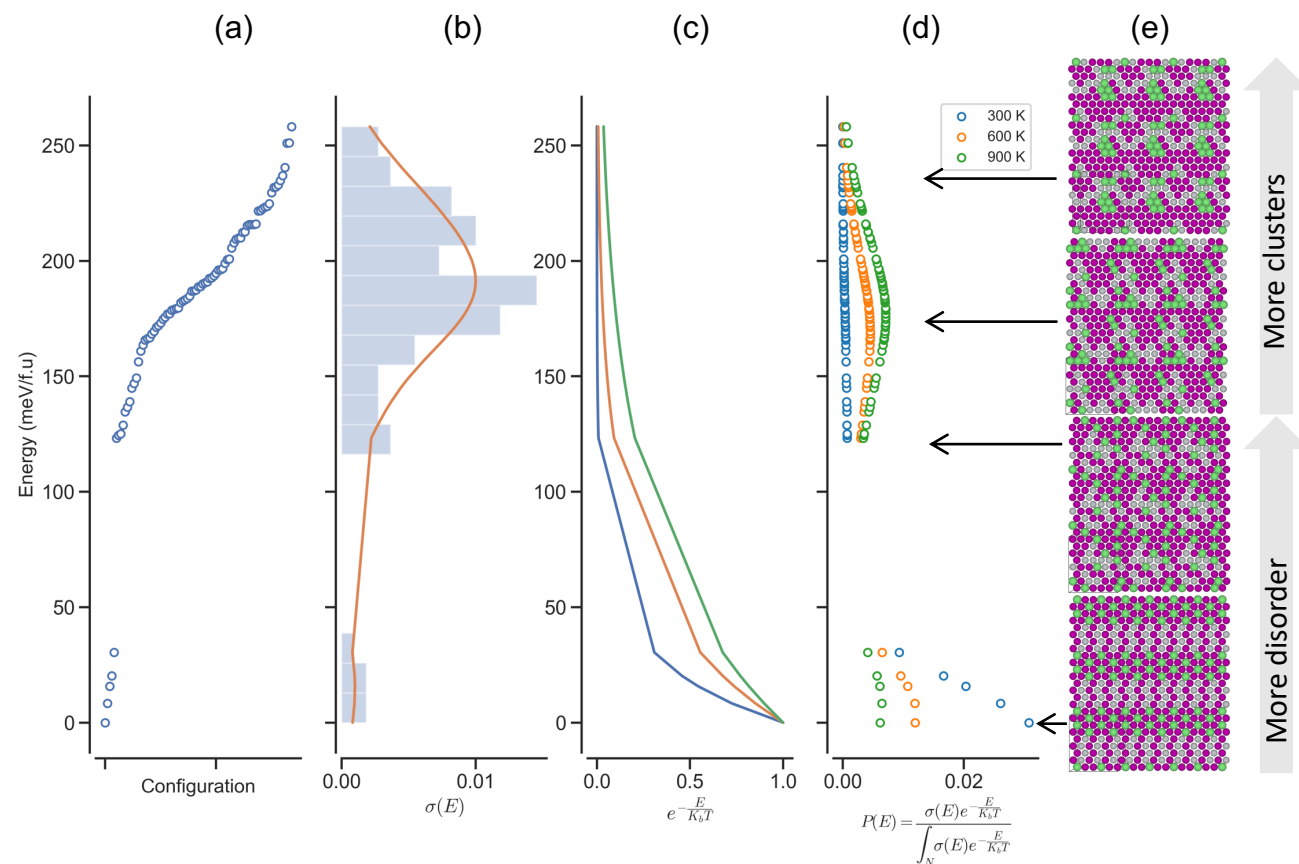
A combined ⁶Li NMR and DFT calculations were used to elucidate the spectral difference observed from the 15 hours and 1-week LiNi_{0.5}Mn_{0.5}O₂ annealed samples. The major takeaways are:

- The synthesis of LiMn_{0.5}Ni_{0.5}O₂ samples must contain many different configurations that all contribute to the overall NMR spectra.
- Li/Ni mixing is the primary cause of the broadening
- NMR shifts near 1400 ppm do not necessarily emanate from Li in the transition metal layer only, but could result from configurations of Li in the Li layer that are well within the accessible majority distribution

Technical Accomplishments

- The energy landscape is widely spread (250 meV/f.u.), reflecting its sensitivity to the atomic configurations
- The “ordered” domain configuration (ribbon) has the lowest total energy
- Introduction of disorder to the ribbon model increases the energy significantly
- The probability of synthesis of “ordered” configurations is limited, whereas there are many possible random configurations centered around 200 eV/f.u. relative to the ordered configuration energy
- To account for finite temperature effects, the Boltzmann factor is applied to the energy data at three temperatures, see Figure panel c
- The probability of occurrence for each tested configuration is plotted in Figure panel d

Earth abundant dopants in $\text{Li}_2\text{MnO}_3\text{-LiMn}_{0.5}\text{Ni}_{0.5}\text{O}_2$



Energy domain distribution on 60%-LiMn_{0.5}Ni_{0.5}/40%-Li₂MnO₃. (a) Relative energy of randomly distributed species with respect to the composite “ribbon” model, (b) density of configurational states, (c) Boltzmann factor, (d) probability of occurrence for each configuration, (e) schematic representation of species distribution for select configurations, purple, gray, and green circles represent Mn, Ni and Li atoms, respectively

Composite configuration is favored at room temperature, whereas the increased configurational entropy favored more “disordered” configurations at higher temperatures.

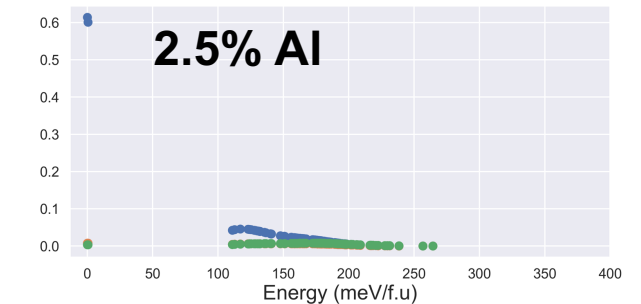
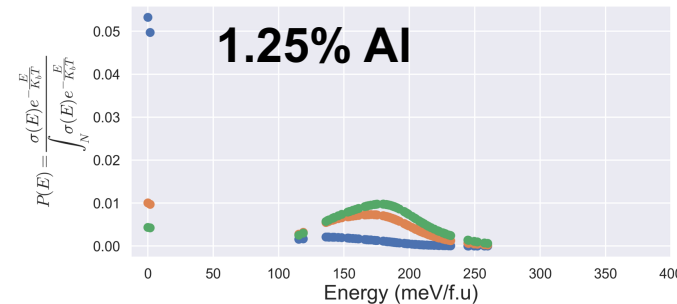
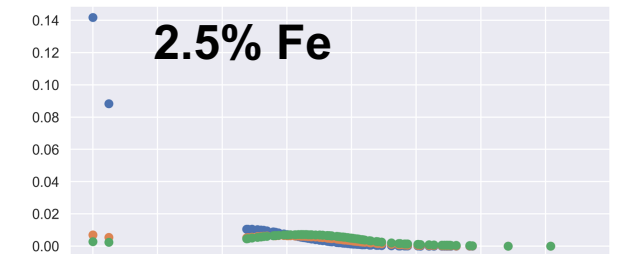
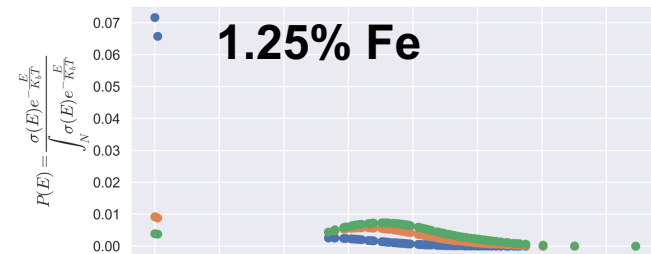
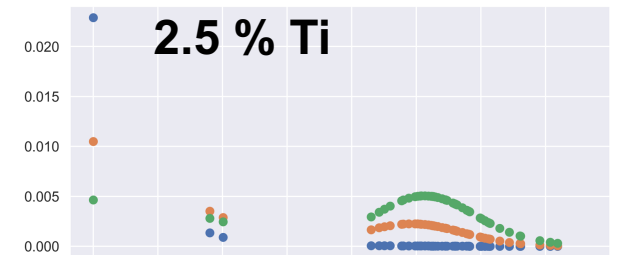
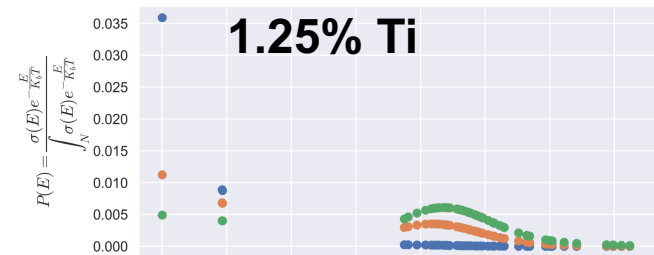
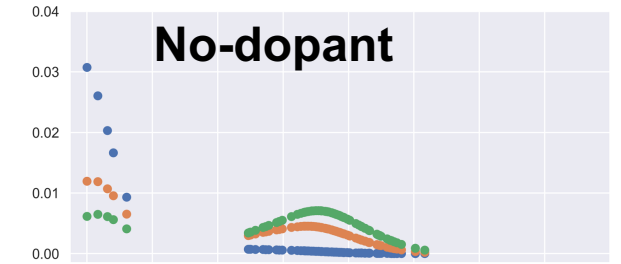
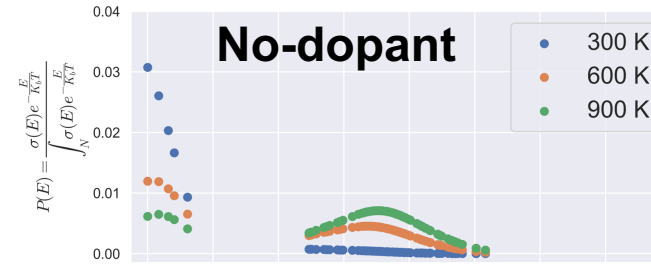
Technical Accomplishments

Effect of dopants on Domain distribution in 60%-LiMn_{0.5}Ni_{0.5} - 40%-Li₂MnO₃

- Higher concentrations of Fe, Al increase the probability of ordered doped configurations. The opposite trend is obtained for Ti
- Disordered configurations have a much lower probabilities with respect to the ordered configurations but increase with increased temperature
- Ti prefers sites in the MnNi zigzag domains
- Al and Fe can be evenly distributed between zigzag and Li₂MnO₃ domains

Earth abundant dopants can disperse Li₂MnO₃ domains.

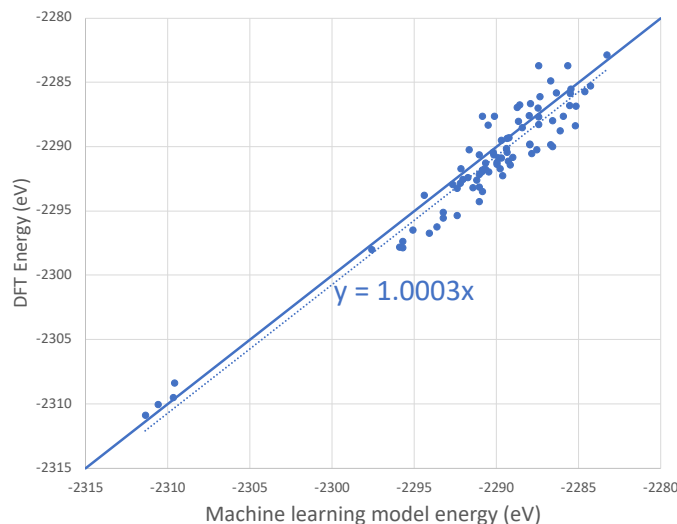
Earth abundant dopants in Li₂MnO₃-LiMn_{0.5}Ni_{0.5}O₂



Technical Accomplishments

Energy estimation for larger cells is needed to reach relevant domain sizes

Machine learning model validation



The model maximum error is less than 4 eV for the cell (10 meV/formula unit)

DFT data

Fit a surrogate model
 $E=f(R)$
 R = atoms coordinates
 Deep learning model

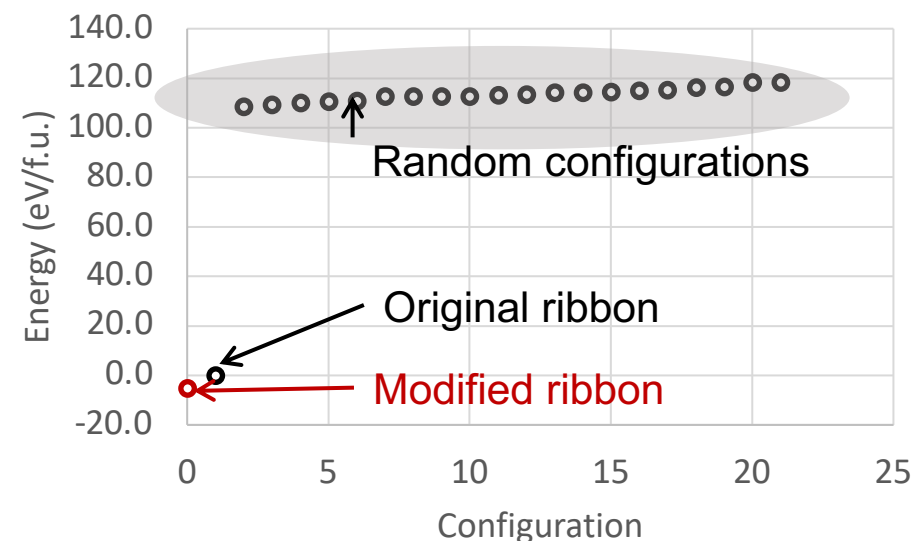
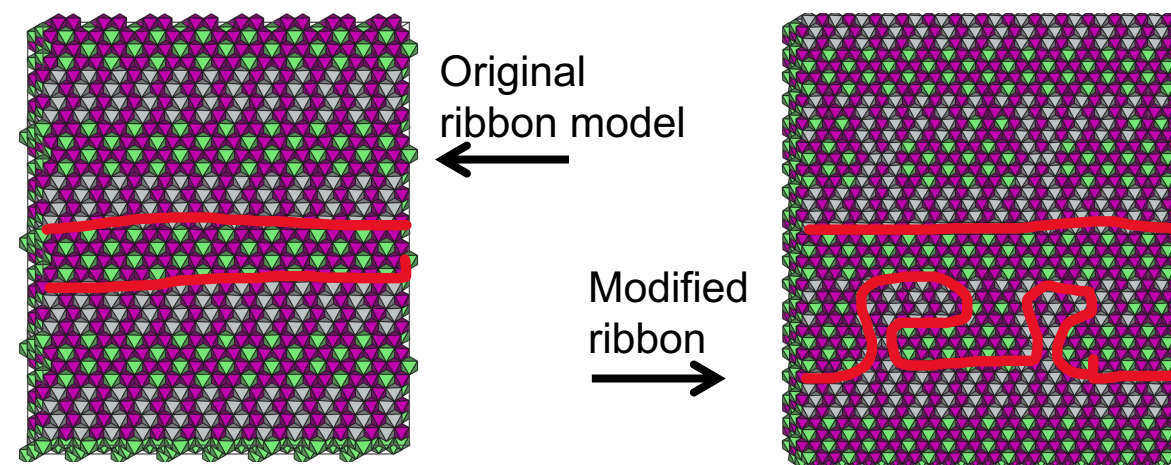
Generate thousand of large simulations cells (6144 atoms)

Compute energy using surrogate model $E(R)$

Low energy configuration + Statistical analysis

Repeat for each dopant

Earth abundant dopants in $\text{Li}_2\text{MnO}_3\text{-LiMn}_{0.5}\text{Ni}_{0.5}\text{O}_2$



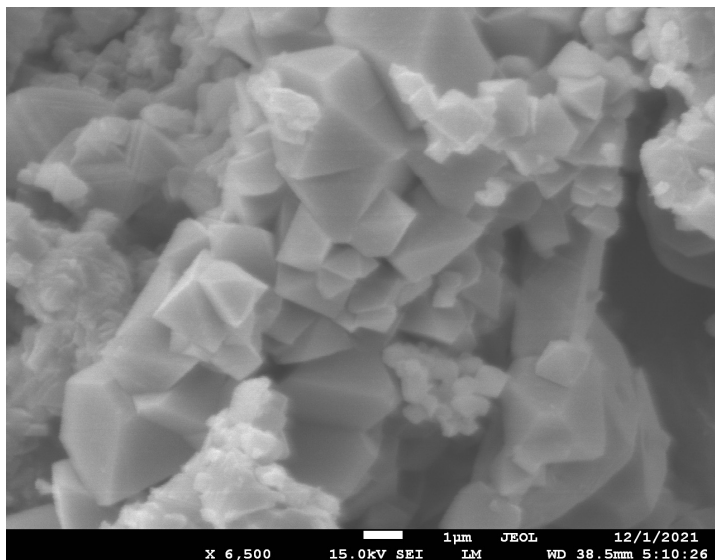
- One modified ribbon model (connected Li_2MnO_3 domains) presented a lower energy than the original model (within the error of the ML model)
- The ML model is being used to predict the optimum Li_2MnO_3 domain size for undoped and doped compositions

Technical Accomplishments

Single-crystal models: Synthesis optimization

Slides from: Guoying Chen LBNL

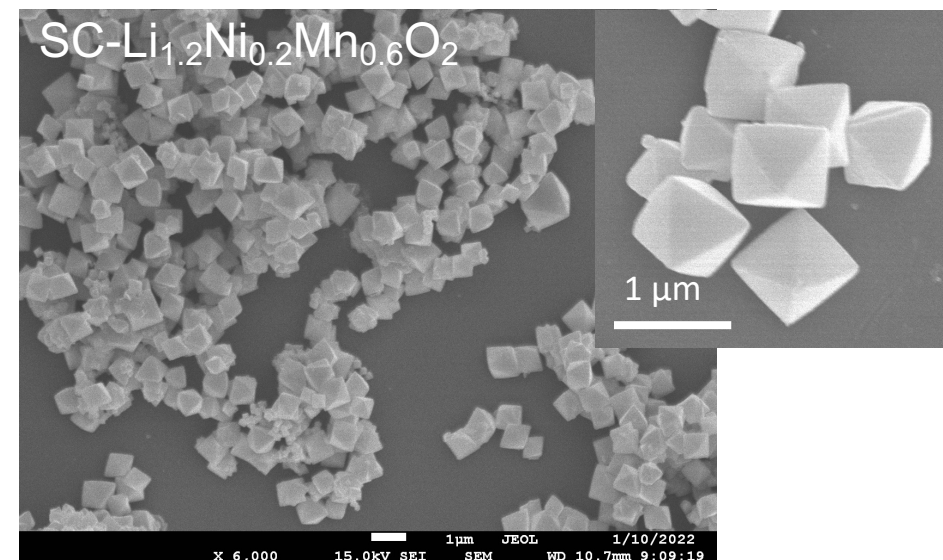
Before synthesis optimization



Modification of
molten-salt
synthesis
conditions



After synthesis optimization



- Non-uniform size and shape
- A few hundred nm to a few μm

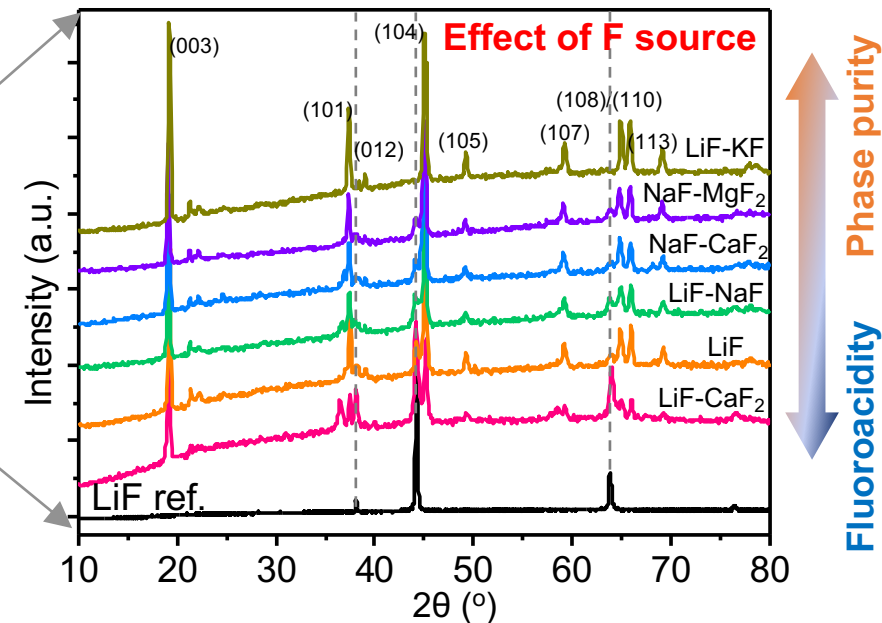
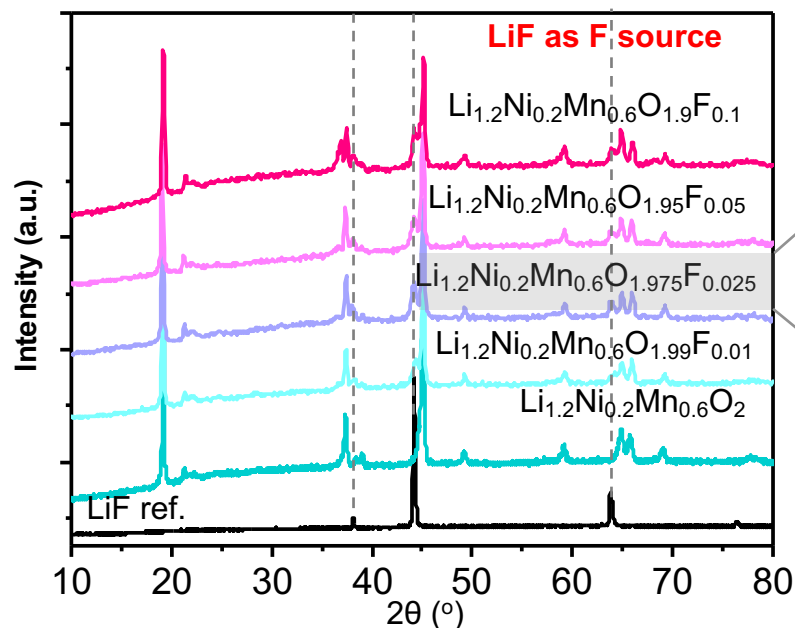
- Uniform size and shape
- Octahedron crystals ~ 1 μm in size

Single-crystal (SC) size and morphology distributions depend on the ratio between flux and the precursors, calcination temperature, heating and cooling rates

Technical Accomplishments

Single-crystal models: Fluorination

Slides from: Guoying Chen LBNL



Fluoroacidity of F-containing molten salts

molten-salt mole ratio m.p.	Basic		Acid			
	NaF-KF	LiF-KF	NaF-MgF ₂	NaF-CaF ₂	LiF-NaF	LiF
	40-60	51-49	78-22	69-31	60-40	80-20
	718°C	492°C	835°C	814°C	652°C	848°C

A Bieber et al., Electrochim. Acta 56, 5022 (2011)

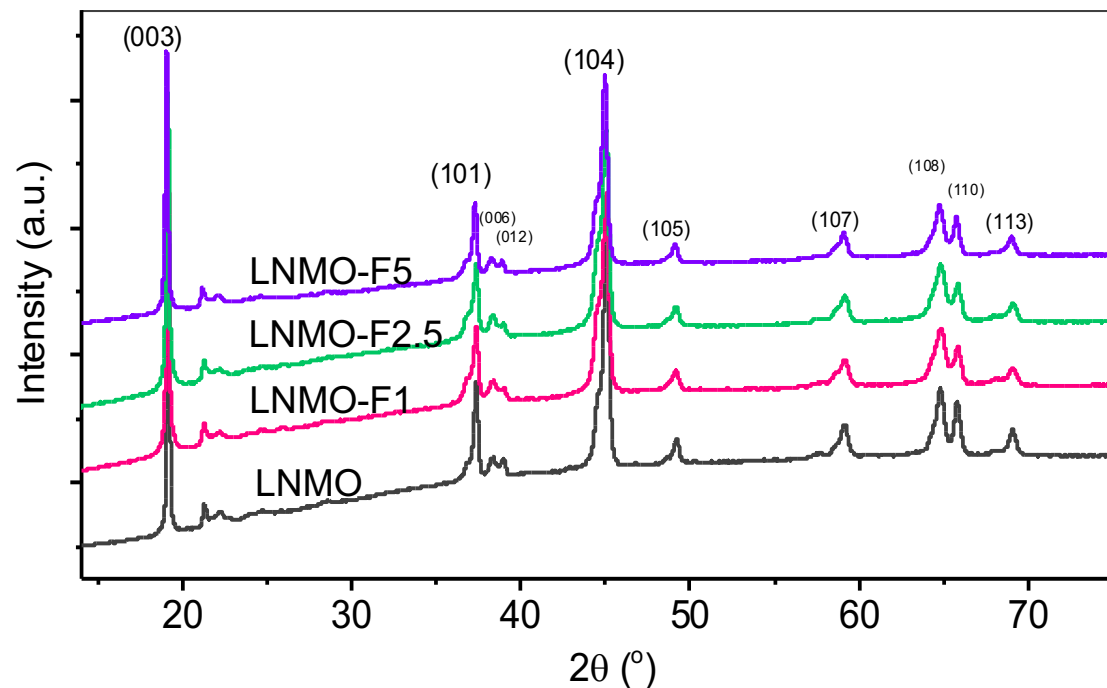
- Fluorobase = fluoroacid + $n\text{F}^-$
- Basic forms are F^- givers, acidic forms are F^- acceptors
- Phase-pure samples are prepared in basic F-systems

SC phase purity depending on Fluoroacidity of the F precursor

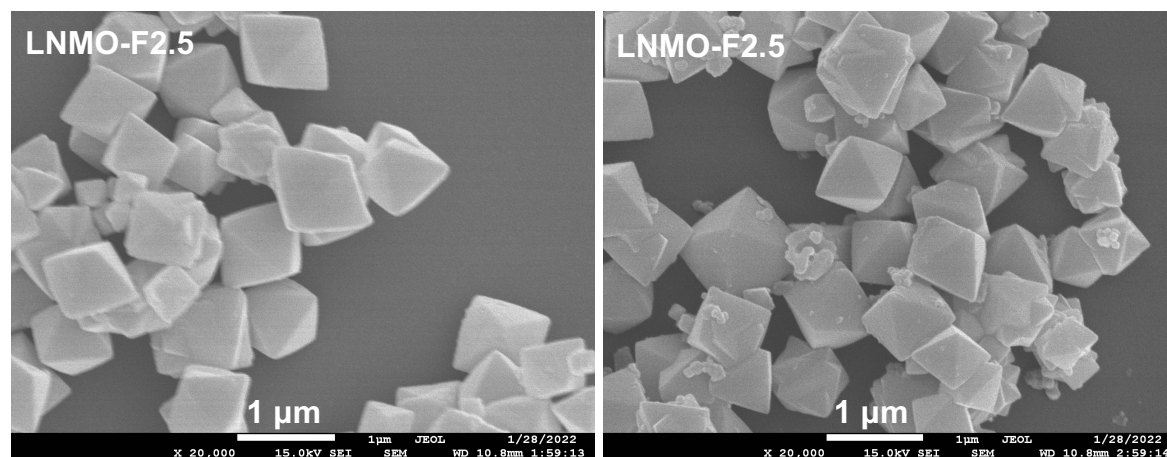
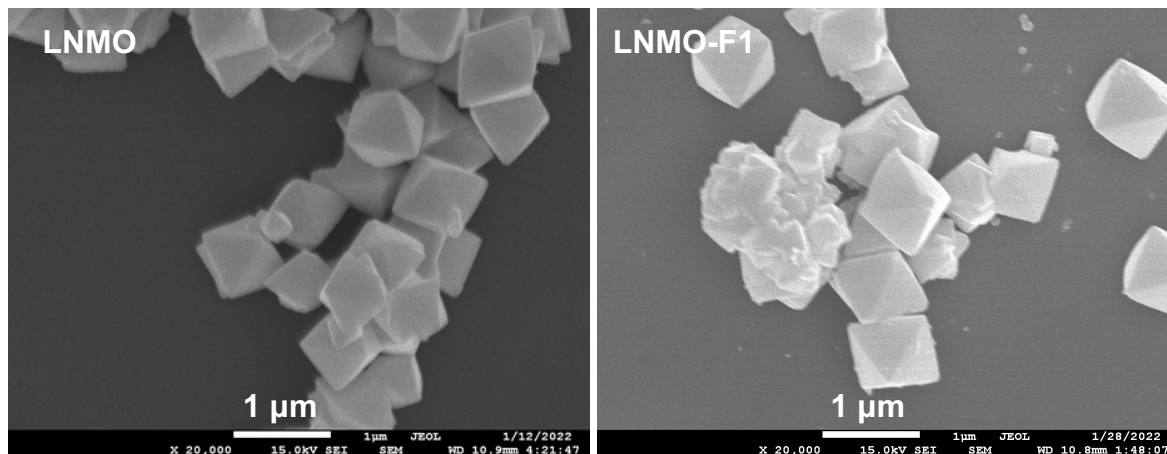
Technical Accomplishments

Single-crystal models: Fluorination

Slides from: Guoying Chen LBNL



Sample label	Target composition	Metal content (ICP)		
		Li	Ni	Mn
LNMO	$\text{Li}_{1.2}\text{Ni}_{0.2}\text{Mn}_{0.6}\text{O}_2$	1.20	0.189	0.611
LNMO-F1	$\text{Li}_{1.2}\text{Ni}_{0.2}\text{Mn}_{0.6}\text{O}_{1.99}\text{F}_{0.01}$	1.19	0.19	0.61
LNMO-F2.5	$\text{Li}_{1.2}\text{Ni}_{0.2}\text{Mn}_{0.6}\text{O}_{1.975}\text{F}_{0.025}$	1.22	0.21	0.59
LNMO-F5	$\text{Li}_{1.2}\text{Ni}_{0.2}\text{Mn}_{0.6}\text{O}_{1.95}\text{F}_{0.05}$	1.22	0.22	0.58

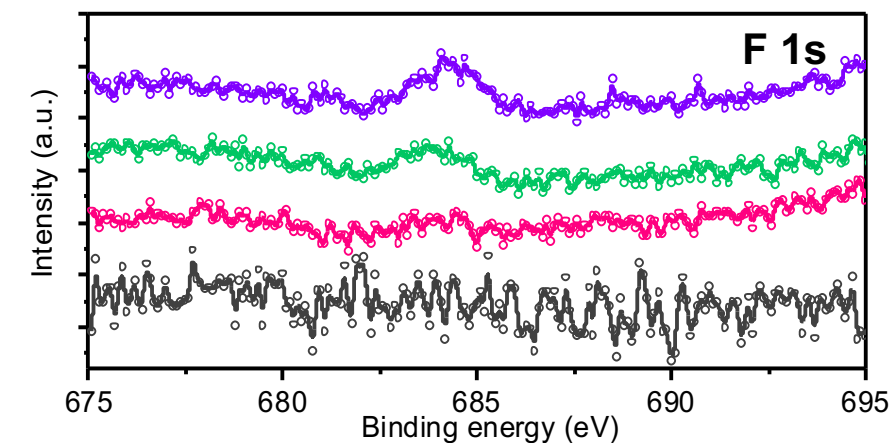
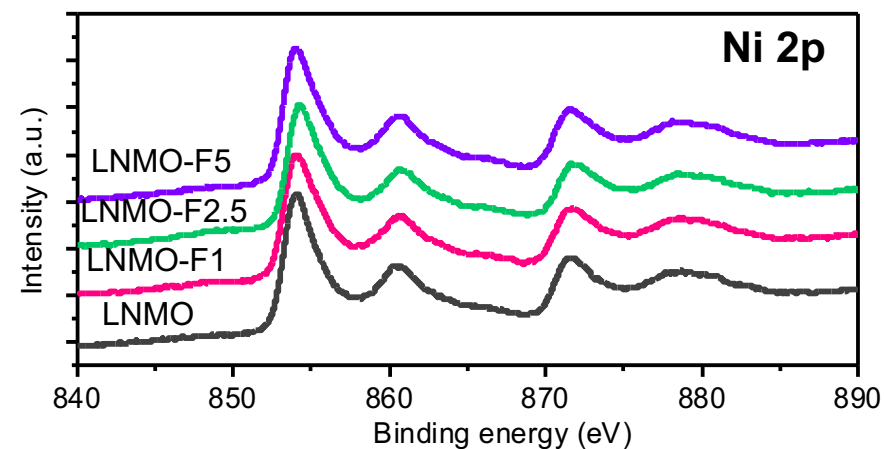
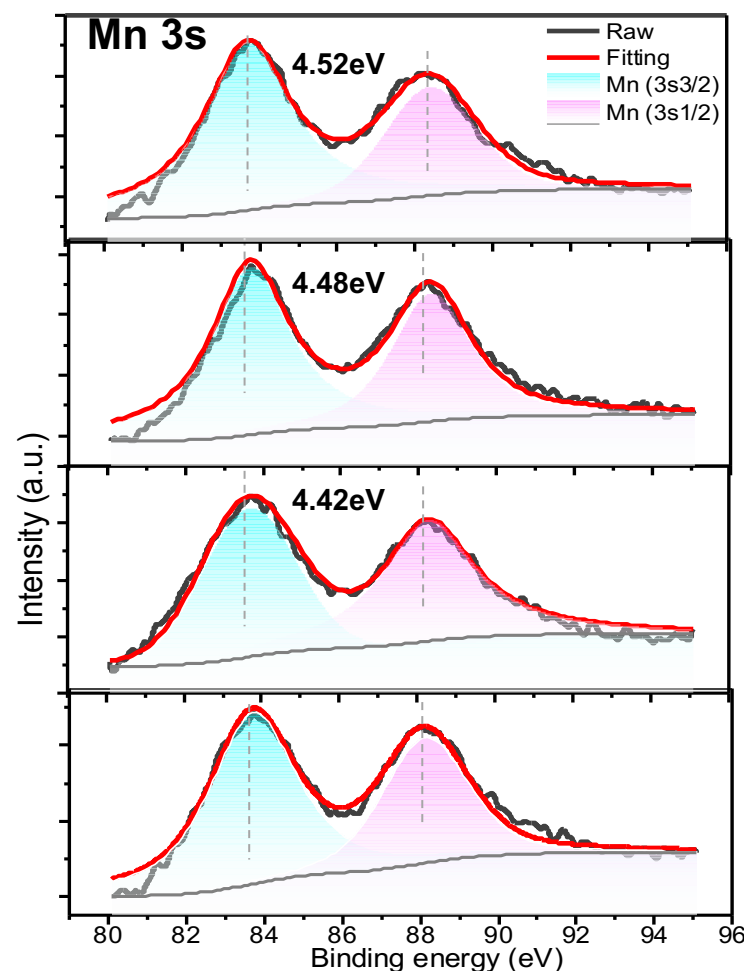
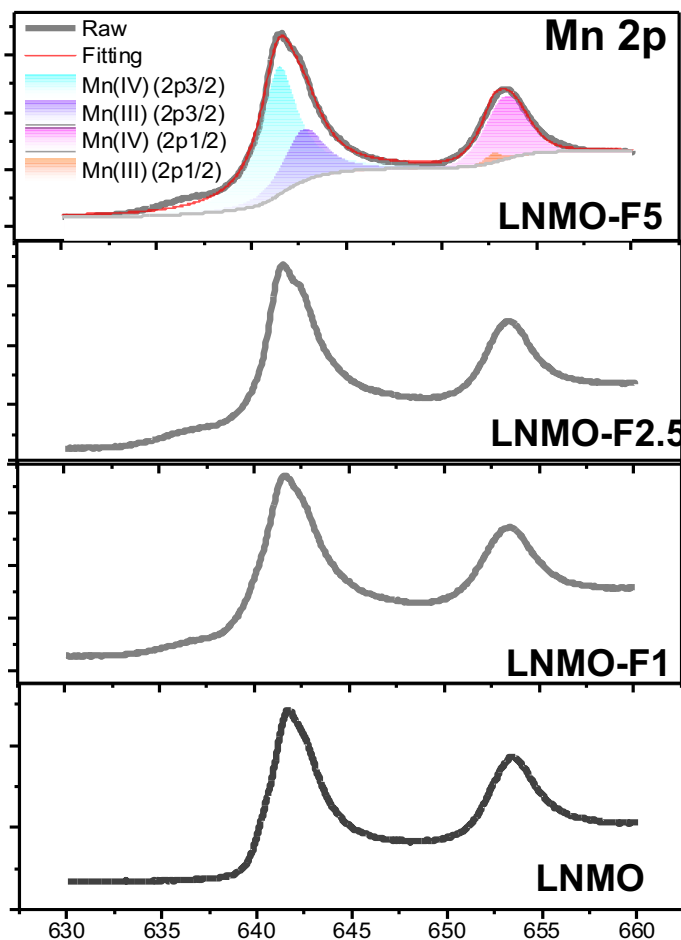


Phase-pure SC samples with various levels of fluorination synthesized with the same uniform size and morphology

Technical Accomplishments

Single-crystal models: Chemical analysis

Slides from: Guoying Chen LBNL



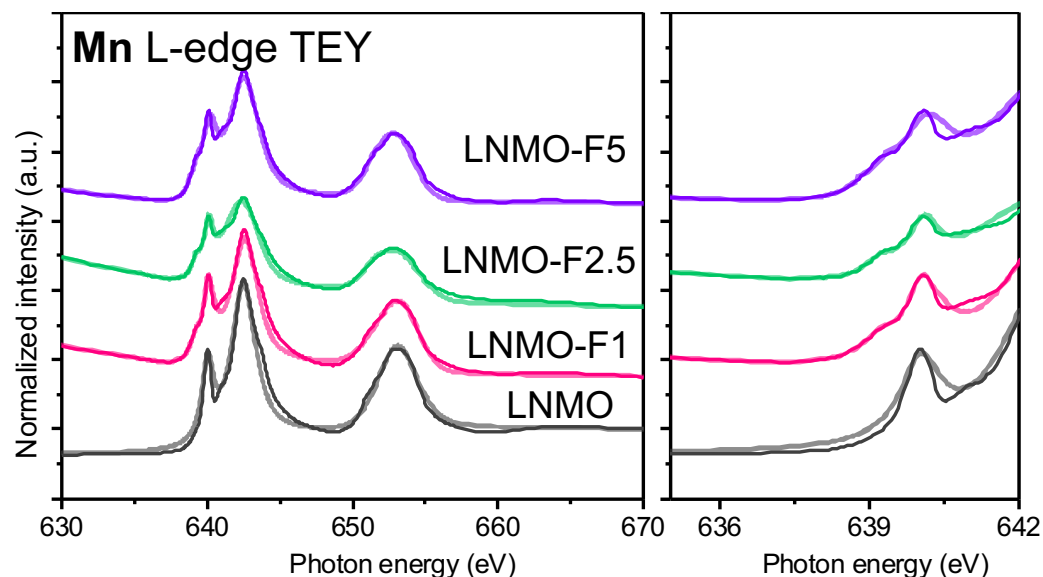
Fluorination leads to the presence of Mn³⁺ on the surface

- No changes in Ni valence
- Weak F signal with broad peaks detected on LNMO-F2.5 and LNMO-F5

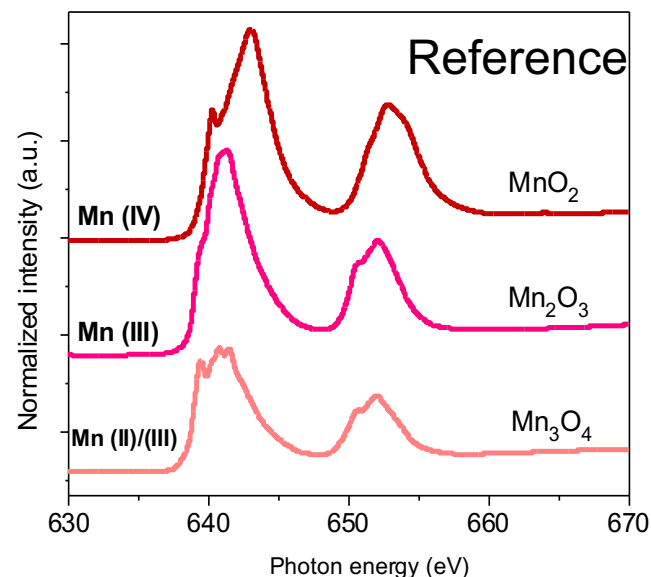
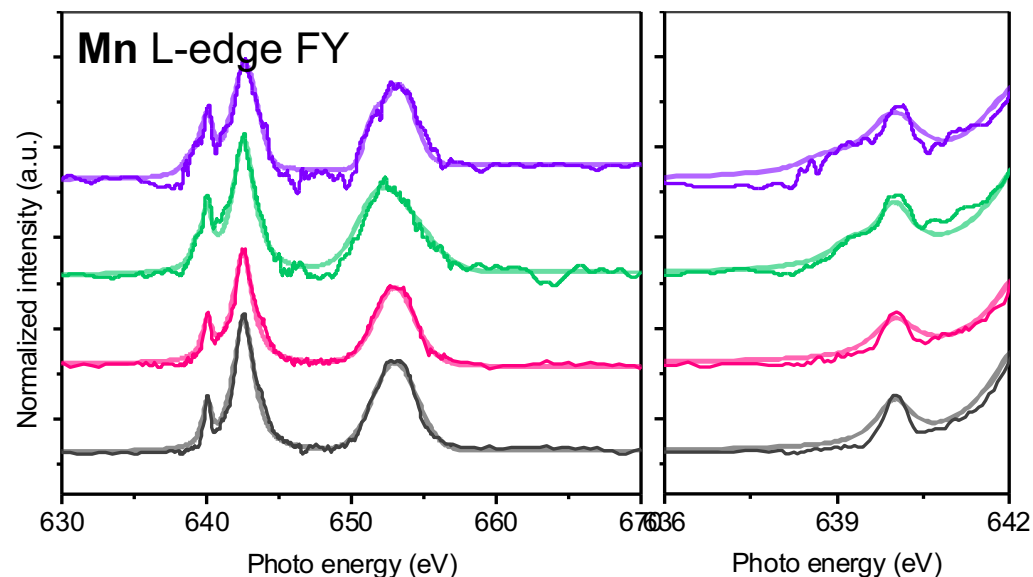
Technical Accomplishments

Single-crystal models: Chemical analysis

Slides from: Guoying Chen LBNL



Mn ³⁺ content	LNMO	LNMO-F1	LNMO-F2.5	LNMO-F5
Calculated (based on F doping level)	0	1.6%	4.2%	8.3%
Estimated (XPS, ~ 2 nm)	0	3%	12%	15%
Estimated (XAS TEY, ~ 5 nm)	0	2.1%	5.1 %	10.4%
Estimated (XAS FY, ~ 50 nm)	0	1.1%	4.9 %	9.1%



- Mn³⁺ content increases with fluorination level
- Mn³⁺ content decreases from surface to bulk
- Gradient Mn³⁺ concentration likely an indication of gradient F distribution from the surface to bulk

Summary

- A combined ^6Li NMR and DFT calculation study was used to better understand the local structures and orderings in $\text{LiNi}_{0.5}\text{Mn}_{0.5}\text{O}_2$: Li/Ni mixing is the primary cause of the NMR broadening; NMR shifts near 1400 ppm do not necessarily emanate from Li in the transition metal layer only, but could result from configurations of Li in the Li layer that are well within the accessible majority distribution.
- The most effective dopants against oxygen reactivity (positive oxygen vacancy formation energy) for the most abundant (012) facet prefer surface sites.
- The less abundant (104) facet is less reactive, and all the dopants investigated so far further improve its stability.
- Composite configuration of 60%- $\text{LiMn}_{0.5}\text{Ni}_{0.5}$ /40%- Li_2MnO_3 is favored at room temperature, whereas the increased configurational entropy favored more “disordered” configurations at higher temperatures.
- Earth-abundant dopants can disperse Li_2MnO_3 domains in 60%- $\text{LiMn}_{0.5}\text{Ni}_{0.5}$ /40%- Li_2MnO_3 .
- Synthesis conditions were optimized and a series of phase-pure LNMO single crystals, with various fluorination levels, prepared prepared.
- Fluorination leads to the presence of Mn^{3+} , with concentration decreasing from surface to bulk
- F concentration likely follows the same surface to bulk distribution as Mn^{3+} . Further analysis underway.

Future Work

Theory

- The influence of earth-abundant elements on surface and bulk integration
- The effects of anion substitutions, the limitations thereof, and the associated electrochemical mechanisms related to anion activity and local order/disorder
- Detailed structural investigations utilizing NMR and X-ray techniques, coupled with machine learning, to predict the overall structure of oxide compositions starting at the atomic level.
- Controlling synthesis conditions in pursuit of compositional and morphological control

Model Systems

- Synthesis and fluorination of LMR particles with different particle morphologies
- Further analysis on F doping level and F distribution at the particle-level
- Evaluation of F effect on electrochemical performance, O loss at high voltages, surface reconstruction and impedance

Any proposed future work is subject to change based on funding levels

Next-Gen Cathode Project Contributors

Collaboration and Coordination

- | | | |
|------------------------------|-----------------------|--------------------------------|
| ▪ Daniel Abraham | ▪ Sang-Don Han | ▪ Boyu Shi |
| ▪ Khalil Amine | ▪ Hakim Iddir | ▪ Woochul Shin |
| ▪ Pavan Badami | ▪ Andrew Jansen | ▪ Ilya Shkrob |
| ▪ Mahalingam Balasubramanian | ▪ Christopher Johnson | ▪ Seoung-Bum Son |
| ▪ Ilias Belharouak | ▪ Ozge Kahvecioglu | ▪ Robert Tenent |
| ▪ Ira Bloom | ▪ Minkyung Kim | ▪ Adam Tornheim |
| ▪ Guoying Chen | ▪ Eungje Lee | ▪ Stephen Trask |
| ▪ Jiajun Chen | ▪ Chen Liao | ▪ Bertrand Tremolet de Villers |
| ▪ Jason Croy | ▪ Wenquan Lu | ▪ John Vaughey |
| ▪ Pragathi Darapaneni | ▪ Mei Luo | ▪ Anh Vu |
| ▪ Dennis Dees | ▪ Anil Mane | ▪ Bingning Wang |
| ▪ Fulya Dogan | ▪ Kyusung Park | ▪ Chongmin Wang |
| ▪ Alison Dunlop | ▪ Saran Pidaparthi | ▪ Faxing Wang |
| ▪ Jeff Elam | ▪ Bryant Polzin | ▪ David Wood |
| ▪ Sarah Frisco | ▪ Andressa Prado | ▪ Zhenzhen Yang |
| ▪ Juan Garcia | ▪ Krzysztof Pupek | ▪ Junghoon Yang |
| ▪ Linxiao Geng | ▪ Yan Qin | ▪ Haotian Zheng |
| ▪ Jihyeon Gim | ▪ Marco Rodrigues | ▪ Peng Zuo |
| ▪ Arturo Gutierrez | ▪ Aryal Shankar | |
| ▪ Jinhyup Han | ▪ Jaswinder Sharma | |

Major Research Facilities

- | | | |
|---|--|---|
| ▪ Materials Engineering Research Facility | ▪ Advanced Light Source | ▪ National Energy Research Scientific Computing Center (LBNL) |
| ▪ Post-Test Facility | ▪ Battery Manufacturing Facility | ▪ Stanford Synchrotron Radiation Light Source |
| ▪ Cell Analysis, Modeling, and Prototyping | ▪ Advanced Photon Source (APS) | |
| ▪ Spallation Neutron Source | ▪ Laboratory Computing Resource Center (ANL) | |
| ▪ Environmental Molecular Sciences Laboratory | ▪ NMR Spectroscopy Lab (ANL) | |

Support for this work from the ABR Program, Office of Vehicle Technologies, DOE-EERE, is gratefully acknowledged – Peter Faguy, David Howell

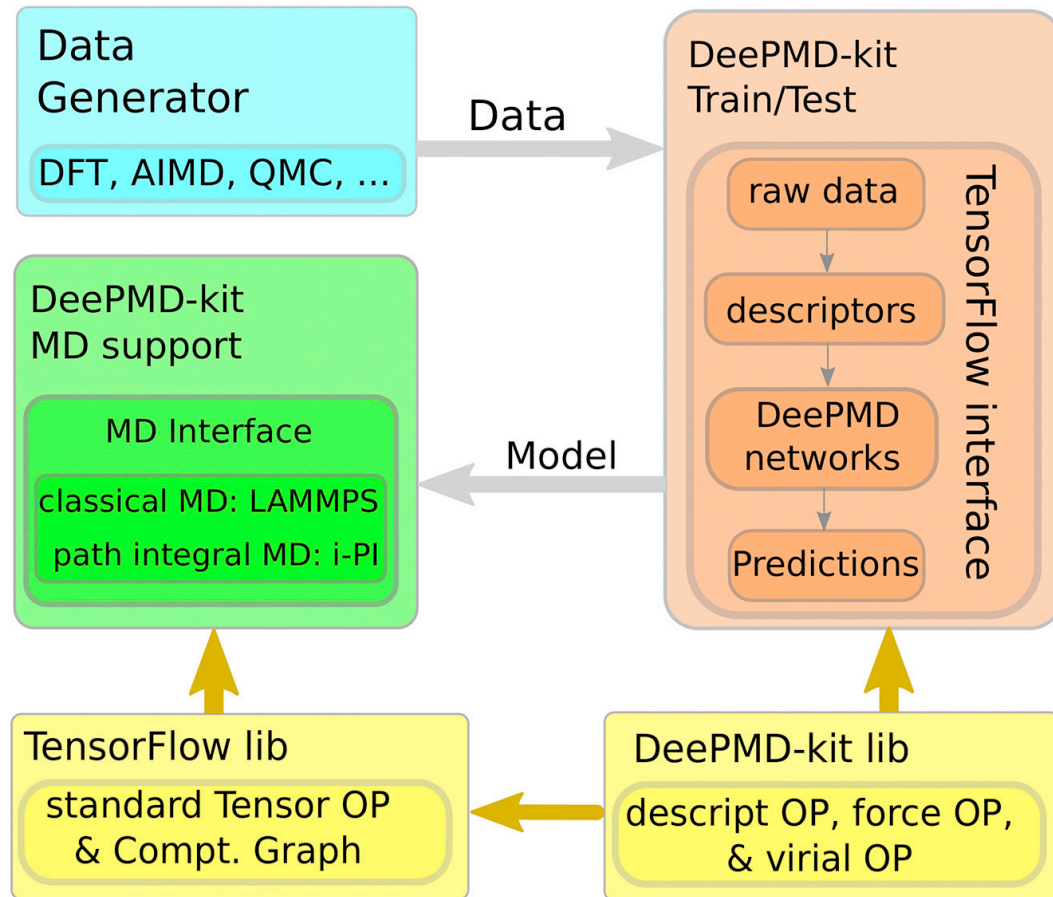
Technical Backup Slides

Technical Backup Slides

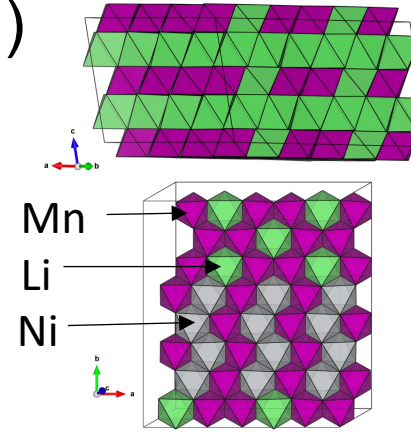
Earth abundant dopants in Li_2MnO_3 -MN5050

Li_2MnO_3 domain size estimation

Machine Learning Potential (surrogate model)



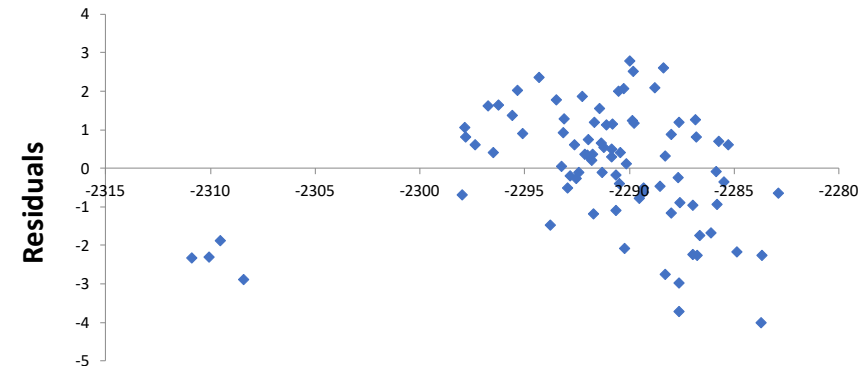
Han Wang, Linfeng Zhang, Jiequn Han, Weinan E. DeePMD-kit: A deep learning package for many-body potential energy representation and molecular dynamics. Computer Physics Communications. 2018, 228, 178-184



→ Density functional theory at GGA+U level was used to generate the training data

→ This cell has **60%/40% MN5050/ Li_2MnO_3** ratio.

→ Use this ribbon model as a starting point to produce a large number of disordered configurations and compare energies.

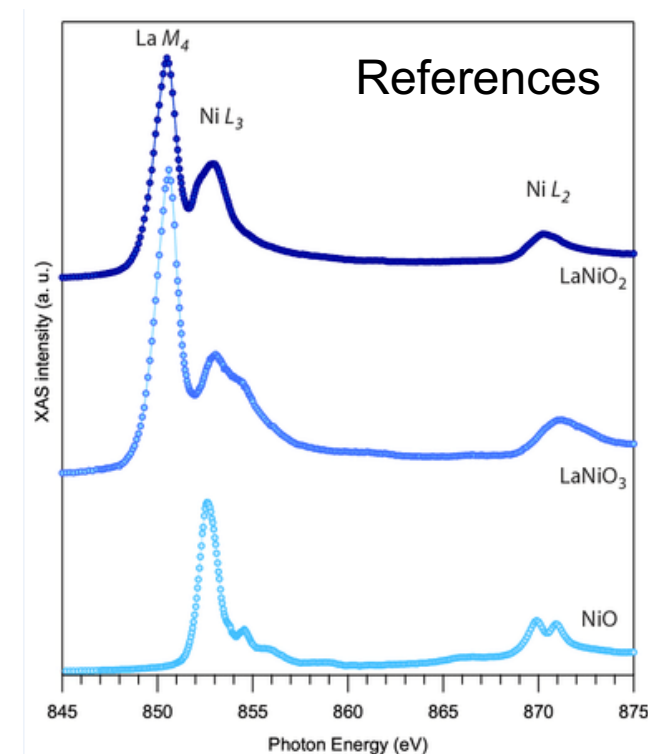
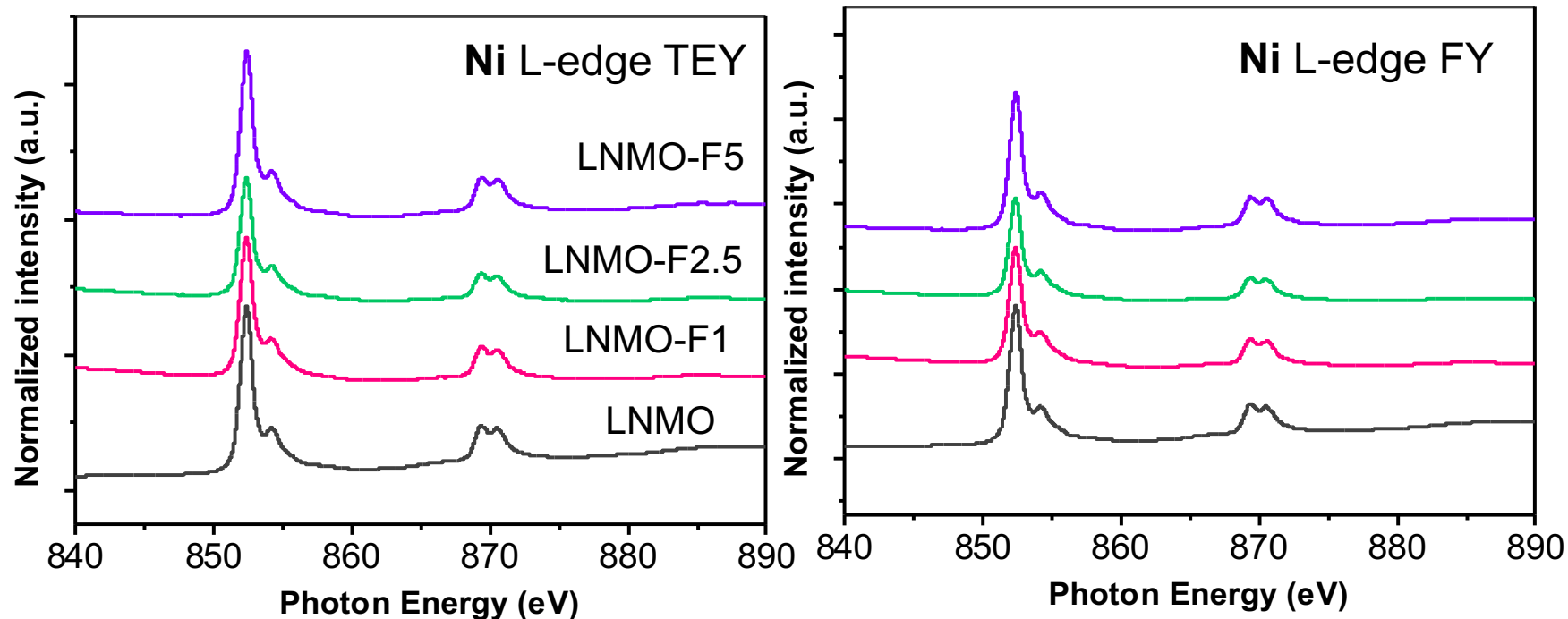


- The model maximum error is less than 4 eV for the cell (10 meV/f.u.)
- The model can compute the total energy in a few seconds for the original cell and about one hour for the 6144 atoms cell

Technical Backup Slides

Single-crystal models: Chemical analysis

Slides from: Guoying Chen LBNL



Ni at 2+ in all samples, shown in both TEY and FY

Nat. Mater. 2020, 19, 381

Patents, Presentations & Publications

- Shin, W.; Garcia, J. C.; Vu, A.; Ji, X.; Iddir, H.; Dogan, F. “Understanding Lithium Local Environments in $\text{LiMn}_{0.5}\text{Ni}_{0.5}\text{O}_2$ Cathodes: A DFT-Supported ^6Li Solid-State NMR Study”. *J. Phys. Chem. C* **2022**, 126 (9), 4276–4285.
- Jianzhong Yang, Marco-Tulio Fonseca Rodrigues, Seoung-Bum Son, Juan C Garcia, Kewei Liu, Jihyeon Gim, Hakim Iddir, Daniel P Abraham, Zhengcheng Zhang, Chen Liao: “Dual-Salt Electrolytes to Effectively Reduce Impedance Rise of High-Nickel Lithium-Ion Batteries”. *ACS Applied Materials & Interfaces* 2021, 13, 34, 40502–40512.
- Anil U Mane, Jeffrey W Elam, Arturo Gutierrez, Jihyeon Gim, Devika Choudhury, Eungje Lee, Hakim Iddir: “Modification of lithium ion electrode materials via atomic layer deposition techniques”, U.S. Patent US Patent App. 16/855,676, (2021).
- Y. Lu and G. Chen, “Methods of Synthesizing Single-Crystal $\text{LiNi}_x\text{Mn}_y\text{Co}_{1-x-y}\text{O}_2$ Cathode Materials,” U.S. Patent Application Ser. No: 63/210,335 (2021).
- M. Kim, L. Zou, S.-B. Son, I. D. Bloom, C. Wang and G. Chen, “Improving LiNiO_2 Cathode through Particle Design and Optimization,” *submitted* (2022).